ARL-TR-8995 ● JULY 2020

DEVCOM ARMY RESEARCH LABORATORY

# A High-Voltage Capacitor Bank Design with a Built-in Spark Gap Switch

by Paul R Berning and Peter T Bartkowski

## NOTICES

### Disclaimers

The findings in this report are not to be construed as an official Department of the Army position unless so designated by other authorized documents.

Citation of manufacturer's or trade names does not constitute an official endorsement or approval of the use thereof.

Destroy this report when it is no longer needed. Do not return it to the originator.

ARL-TR-8995 ● JULY 2020


# A High-Voltage Capacitor Bank Design with a Built-in Spark Gap Switch

**Paul R Berning and Peter T Bartkowski**
*Weapons and Materials Research Directorate, CCDC Army Research Laboratory*

# REPORT DOCUMENTATION PAGE

*Form Approved*
*OMB No. 0704-0188*



| 1. REPORT DATE *(DD-MM-YYYY)* | 2. REPORT TYPE | 3. DATES COVERED (From - To) |
|---|---|---|
| July 2020 | Technical Report | 1 February–3 July 2020 |

**4. TITLE AND SUBTITLE**
A High-Voltage Capacitor Bank Design with a Built-in Spark Gap Switch

**5a. CONTRACT NUMBER**

**5b. GRANT NUMBER**

**5c. PROGRAM ELEMENT NUMBER**

**6. AUTHOR(S)**
Paul R Berning and Peter T Bartkowski

**5d. PROJECT NUMBER**

**5e. TASK NUMBER**

**5f. WORK UNIT NUMBER**

**7. PERFORMING ORGANIZATION NAME(S) AND ADDRESS(ES)**
CCDC Army Research Laboratory
ATTN: FCDD-RLW-PA
Aberdeen Proving Ground, MD 21005-5066

**8. PERFORMING ORGANIZATION REPORT NUMBER**
ARL-TR-8995

**9. SPONSORING/MONITORING AGENCY NAME(S) AND ADDRESS(ES)**

**10. SPONSOR/MONITOR'S ACRONYM(S)**

**11. SPONSOR/MONITOR'S REPORT NUMBER(S)**

Approved for public release; distribution is unlimited.

**13. SUPPLEMENTARY NOTES**
ORCID ID(s): Paul Berning, 0000-0001-9699-0245

**14. ABSTRACT**
A 20-kV, 38-kJ capacitor bank with a built-in spark gap switch was designed, built, and tested. Currents in excess of 400 kA were achieved. The motivation for the design, the details of the design, and the results of testing are described.

**15. SUBJECT TERMS**
pulsed power, spark gap switches, energy storage capacitors, electrothermal launchers, high voltage

| 16. SECURITY CLASSIFICATION OF: | | | 17. LIMITATION OF ABSTRACT | 18. NUMBER OF PAGES | 19a. NAME OF RESPONSIBLE PERSON |
|---|---|---|---|---|---|
| a. REPORT | b. ABSTRACT | c. THIS PAGE | | | Paul R Berning |
| Unclassified | Unclassified | Unclassified | UU | 41 | 19b. TELEPHONE NUMBER (Include area code) (410) 278-4509 |

## Contents

## List of Figures

## List of Tables

## Acknowledgments

The authors thank Ronald Cantrell, Corey Yonce, and Robert Borys Sr for their aid in constructing and testing the power supply. They also thank Dr Michael Zellner for reviewing the manuscript.

# 1. Introduction

The pulsed-power energy source described in this report was meant to replace a laboratory setup in which a particular type of miniature electrothermal (ET) launcher was attached to high-voltage (HV) energy storage capacitors by means of a mechanical switch. The ET launchers, which were developed at the US Army Combat Capabilities Development Command (CCDC) Army Research Laboratory (ARL), require a fast risetime and a high peak current.[1–3] A mechanical switch was originally chosen because it introduces very little inductance into the circuit, allowing for peak currents as high as 400 kA.

The mechanical switch was not conducive to precise timing or activation from remote locations, however, limiting its utility outside the laboratory setting. Thus, it was decided to build a system that incorporated a triggerable, high-current spark gap switch in its place. Since spark gap switches have specific needs in regard to how current is fed into and out from them, and there was a strict need to minimize the inductance of those connections in this application, it was decided that making the switch part of the capacitor bank header itself made sense.

While the amount of stored energy in the ET gun power supply is a modest 38 kJ, 400 kA is a considerable amount of current. As such, a spark gap switch design with robust graphite electrodes was chosen. The robustness of the electrodes was assessed in a separate test bed prior to construction of the final capacitor bank. The results of those experiments are also described.

The test stand that served as the ET gun mount has been used for other work, such as exploding foil and exploding wire experiments, so the switched power supply should be useful in a variety of other circumstances as well.

# 2. Legacy Configurations

## 2.1 Capacitor Technology

A variety of capacitor technologies exist, each suited for particular uses. HV energy storage capacitors generally come in two forms, one that uses a pair of thin foils separated by a dielectric layer, and one that uses thin metal layers vacuum deposited directly onto both sides of a thin plastic film.

In one of most common types of foil capacitor, long strips of aluminum foil are separated by a long strip of kraft paper; the layered strips are formed into a roll; the roll is inserted into a sheet metal can; and the can is backfilled with an insulating

oil. Once the oil impregnates the kraft paper, it becomes a crucial part of the capacitor's dielectric.

Metal foil capacitors have advantages and disadvantages. One advantage is that it is relatively easy to make electrical connection to the foils and relatively easy to extract large currents from them. The main disadvantage of foil capacitors is their failure mode: eventually a short will form somewhere in a capacitor roll and, because the foils can support relatively large currents, much of the stored energy can be rapidly deposited at that location. The result often resembles an explosion. The amount of damage that occurs depends on the amount of energy in the system. Some systems that incorporate foil capacitors connect to them via high-energy fuses or resistors to limit the amount of current that will flow if one of the capacitors fails.

Foil/kraft-paper capacitors also tend to have poor energy densities, which is to say they are bulky and heavy. Despite these disadvantages, foil/kraft-paper capacitors are still manufactured and sold, as they are relatively inexpensive to make and have high current capability. That said, metallized film capacitors have largely replaced foil capacitors in most DC and 50-/60-Hz AC applications.[4]

Metallized film capacitors[4,5] are a more modern alternative to foil/kraft-paper capacitors. In this technology, microscopically thin layers of aluminum are deposited onto thin plastic film, typically polypropylene (PP), a roll (or rolls) formed, end connections made, roll (or rolls) inserted into a sheet metal can, and the can is backfilled with oil, typically vegetable oil or mineral oil. In this case, the oil does not impregnate the rolls of metallized plastic film; it is there to prevent the aluminum metallization from oxidizing and to help electrically insulate the internal connections.

If the capacitors are packaged to maximize energy density, metallized film capacitors can exhibit the highest energy densities available in HV energy storage capacitors—1 to 3 J/cc if PP film is used. However, the highest energy densities are typically only found in capacitors with high internal inductance and low current capability, which are only suited for pulses whose periods are measured in milliseconds. Optimized "short-pulse" capacitors, those with low internal inductance and thus suited for pulses with periods that are a small fraction of a millisecond, typically have energy densities between 0.9 and 1.2 J/cc.[4,5]

The main advantage of metallized film capacitors is that they fail in a benign fashion. Shorts between the two layers of metal film in a metallized film capacitor do not cause massive destruction. Since the metal layer is so thin, it only takes a tiny bit of energy to evaporate a small region of metal surrounding the short, thereby "clearing" an area around it and isolating it from the rest of the system. Metallized film capacitors are referred to as "self-healing" for this reason.[4,5]

The number of "cleared" regions increases over the lifetime of the capacitor. In particular, the number increases when the capacitor sits at HV for long periods and every time a high-current pulse is extracted. Eventually, the cleared regions join and isolate entire sections of film, reducing overall capacitance.[4,5] As more damage is incurred in the metal layer, it reaches a point where it becomes a runaway process and capacitance starts to drop rapidly.

While there is considerable statistical variation in just when that runaway process starts, manufacturers often choose a certain level of capacitance decrease, on the order of 5%, beyond which the capacitor is considered to have "failed". Since both standing at full charge and supplying high-current pulses contributes to the damage, each capacitor design is rated for both "DC life" and "shot life" on that basis. There is also a "fault current" specification that indicates the maximum peak current that can be sustained a few times in the capacitor's lifetime without causing the capacitor to fail entirely.

## 2.2 First-Generation Power Supply

Initially, the power supply for the electrothermal gun consisted of a single General Atomics (GA, San Diego, California; formerly Maxwell) Model 32511 capacitor, pictured in Fig. 1. These capacitors were an older style of metallized-film energy storage capacitor that used PP film, manufactured circa 1990. The particular capacitors used were salvaged from an outside agency and little is known about their history. They have a nominal capacitance of 175 μF and were initially rated for a maximum of 24 kV, representing 50 kJ of stored energy (later versions of this design were downgraded to 22 kV after problems arose). Virtually all of the experiments involving early development of the miniature ET launcher were performed at 20 kV, representing 35 kJ of stored energy.

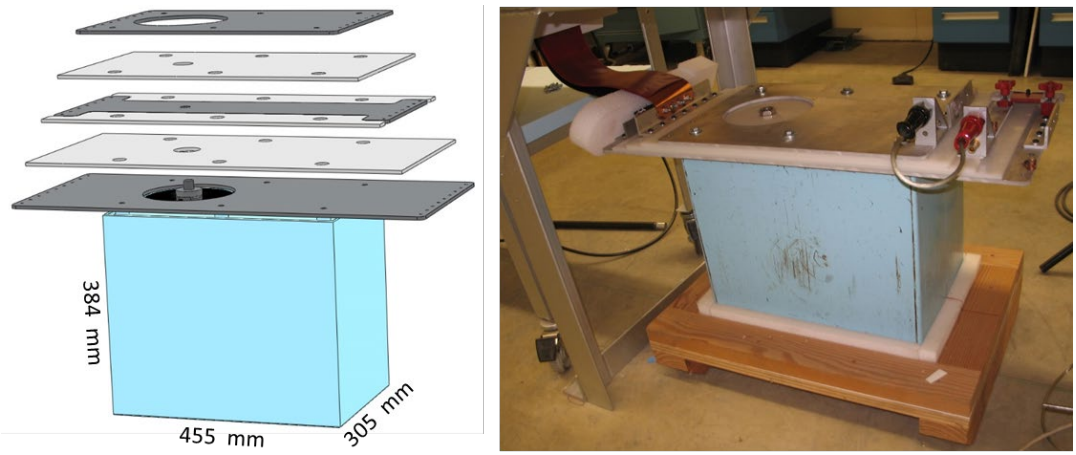


**Fig. 1 Drawing of a GA Model 32511 capacitor with attachment provisions (left) and the same capacitor installed in the laboratory (right)**

The photograph on the right in Fig. 1 shows one such capacitor installed in its laboratory configuration. External connections were made using a low-inductance triplate header layered in a "ground-hot-ground" configuration (depicted on the left in Fig. 1). It was installed under the table that the load was mounted on. Connections to the load were made with the two insulated, 101-mm wide, 0.5-mm-thick copper strips (seen on the left in the photo). Current was measured by a calibrated Rogowski coil enclosed in the foam structure surrounding the ground connection (seen on the left in the photograph). This setup supplied pulses with peak currents in the 350- to 400-kA range and with periods on the order of 40 μs.

The main difficulty with the first-generation power supply was that the capacitor in question was not rated for peak currents of 350 to 400 kA. While no specifications for this model capacitor can be found, this type of capacitor is usually rated for 60- to 100-kA peak current (a similar GA design has a 100-kA rating). As such, extracting a 400-kA pulse from this capacitor has a profound effect on its shot life. While this capacitor may well be capable of supplying hundreds of 100-kA pulses, experience has shown that it is only capable of supplying about eight 400-kA pulses before failing. This is why several such capacitors failed during the early testing phase of the ET gun concept.

The internal resistance of the capacitor was higher than desired as well because, once again, it was not designed to supply 400-kA pulses.

## 2.3 Second-Generation Power Supply

It was then decided to replace the single capacitor with several capacitors to spread the current load over multiple capacitors. Total resistance and inductance can sometimes be reduced in this way as well. It was decided to use three 20-kV, 12.5-kJ capacitors, each rated for 130 kA (still an unusually high current rating for PP film capacitors). A request for quote (RFQ) was issued, and the result was the ICAR Bioenergy Model D 65-B 62.5-2000 capacitor (ICAR S.p.A, Monza, Italy). These capacitors are rated for 300+ h or more DC life and 1,000+ (full specifications can be found in the Appendix).

Three of these capacitors are pictured in Fig. 2 alongside a single GA 32511 capacitor. The main difference between the old and new capacitors is immediately obvious: the ICAR capacitors occupy far more volume. While this is due in part to the high peak-current requirement, which adds extra packaging burdens, it is mostly because few limits were put on the dimensions of the capacitors when the RFQ was written, as these capacitors were only meant for laboratory use.

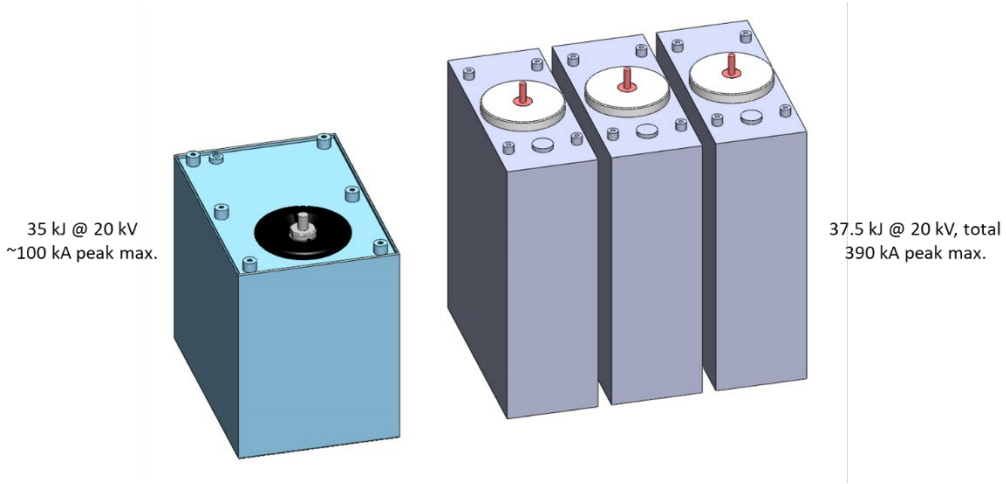


**Fig. 2 GA Model 32511 capacitor (left) and three ICAR Model D 65-B 62.5-2000 capacitors (right)**

Typically, low-inductance, fast-pulse capacitors have energy densities on the order of 0.9 to 1.2 J/cc (the 32511 capacitor has a maximum energy density of 0.9 J/cc). For unknown reasons, the 12.5-kJ ICAR caps have an astonishingly low energy density—0.33 J/cc. The manufacturer likely chose this geometry for ease of construction. For comparison, the authors are aware of another ICAR capacitor model that is rated for peak currents up to 150 kA and yet still maintains an energy density of 0.8 J/cc.

The design of the first capacitor bank to use the new capacitors is illustrated in Fig. 3. It also uses a triplate header configuration, where each of the three

conductive layers is made from 3/8-inch (9.5-mm) 6061 aluminum alloy plate. The insulating layers between the metal plates are made from 3/8-inch (9.5-mm) high-density polyethylene. An aluminum bushing connects the upper and lower ground plates at each mounting bolt location (i.e., at the location of each threaded boss on the capacitors). The output connections are made via a series of threaded holes on one edge of each plate. In general, the loads are typically connected to only one of the two ground plates.

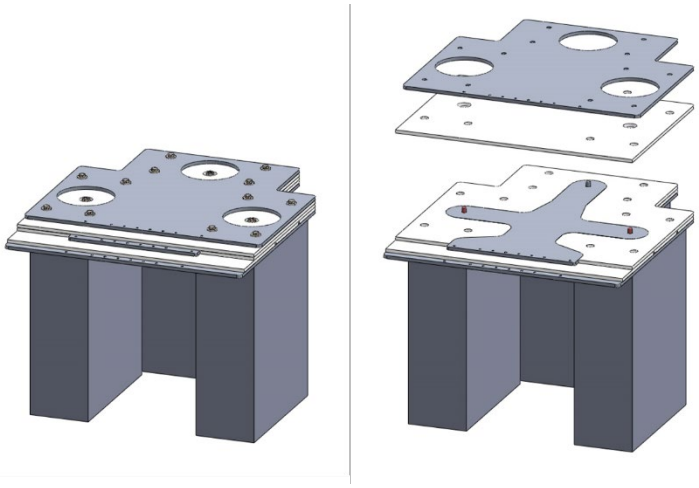

**Fig. 3 Second-generation capacitor bank design**

The fact that this capacitor bank is expected to extract the maximum allowed peak current from each of its capacitors adds an additional design requirement: to assure that the demand on each capacitor is the same, the inductance of the paths between each capacitor's HV stud and the HV output section must be the same. The shape of the middle hot plate seen in Fig. 3 attempts to balance these inductances. Any imbalance will shorten the lifetime of any cap that is overburdened. Note this feature (in conjunction with electrical insulation requirements) drives the positioning of the capacitors and thus adds to the overall volume of the capacitor bank.

The capacitance of this bank proved to be slightly higher than nominally expected—190 μF, representing 38 kJ of stored energy at 20 kV. Figure 4 shows a picture of this bank as it is set up in the laboratory (left). The ET gun mount and mechanical switch are pictured on the right.

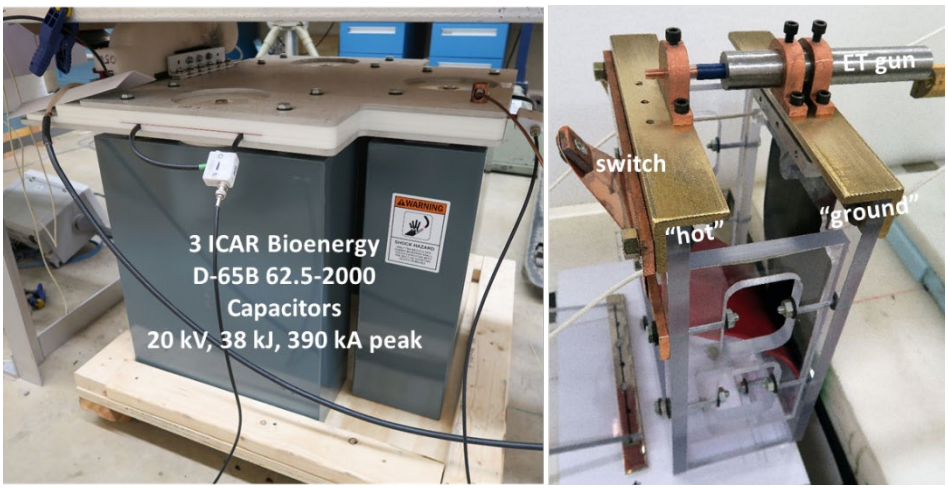


**Fig. 4 Second-generation 38-kJ capacitor bank (left) and gun mount with mechanical switch (right)**

# 3. Capacitor Bank with Built-in Spark Gap Switch

## 3.1 Spark Gap Background

As 400 kA is not an insignificant current, it was decided to follow the example of other high-current spark gap designs and use graphite electrodes.[6] Graphite is superior to any metal in this role, as it exhibits far less erosion.[7]

A prime example of this kind of switch is the commercially available L3 Communications (San Leandro, California; formerly Physics International) ST-300 spark gap switch, pictured in Fig. 5. This is a two-electrode-style switch triggered by overvolting the gap. The switch's specifications are impressive: up to 600-kA peak current, up to 540 C of charge transferred per pulse, and an electrode tip life of 16 kC (https://www2.l3t.com/ati/pdfs/St-300.pdf). It has a coaxial configuration, can be pressurized to change the operating voltage, and has 2.75-inch (70-mm)-diameter field-replaceable graphite electrodes. The gap is enclosed in a solid aluminum "top hat" so the arc byproducts do not damage the fiberglass tube that insulates the switch.

**Fig. 5 L3 Communications ST-300 spark gap switch**

Impressive as it is, this switch has several inconvenient features. First, the switch by itself is claimed to have an inductance of around 200 nH, which is higher than desired for CCDC Army Research Laboratory's ET gun work. ARL's single-barrel ET gun design prefers total circuit inductances between 270 and 350 nH. The switch's awkward connection scheme also makes it difficult to formulate low-inductance connections.

Like all high-current spark gaps, the current needs to be fed into and out of the switch in such a way as to avoid magnetic (i.e., J × B) forces acting on the arc and thereby dragging it off the graphite electrode. This requires feeds that are either run parallel to the arc (and thus generate no J × B) or ones that enter and exit the switch symmetrically from at least two sides (and thus generate no *net* J × B). The switch seen in Fig. 5 illustrates this point handily: the connection scheme pictured is clearly asymmetric, and there is clear evidence of arc damage seen on the inside wall of the aluminum top hat.

Another disadvantage of the stock ST-300 switch is that it is triggered by overvoltage. This is achieved with a short 75-kV pulse generated by the L3 Communications Model TG-75 trigger generator, which is roughly the same size as the switch itself (https://www2.l3t.com/ati/pdfs/Tg-75.pdf). Extra components must be inserted in the circuit to protect the capacitors and any other components that cannot withstand that 75-kV pulse, which greatly complicates the circuit. Furthermore, experience has shown that generation of the 75-kV trigger pulse tends to interfere with nearby electronics.

At ARL, the disadvantages of the triggering scheme were bypassed by the simple expedient of converting the ST-300 to a three-electrode spark gap design of the Trigatron type.[8] This involved drilling a hole in the top of the switch, through the

top electrode, so that an insulated 4-mm-diameter tungsten rod could be inserted until its end was flush with the surface of the top graphite electrode. A Trigatron is triggered by generating a substantial spark between the trigger electrode (i.e., the tungsten electrode) and the main spark gap electrode.

Originally, it was thought that the trigger spark in a Trigatron generates UV light, which in turn ionizes some of the air in the gap and initiates a cascade of ion formation that ultimately leads to an arc discharge. The trigger mechanism proves to be somewhat more complicated than that, however.[8] It has been found that homopolar trigger configurations (i.e., where the polarity of the trigger pulse is the same as the polarity of the adjacent electrode and thus adds to the total voltage across the gap) yield the lowest switch delays. At ARL, we have found that the Trigatron version of the ST-300 switch can be triggered by a 4-kV exploding bridge wire (EBW) firing unit, commonly found on many explosives ranges.

One disadvantage of Trigatrons is that the trigger electrode can erode at a faster rate than the main electrodes. While this is an issue if you expect the switch to transfer 540 C per pulse, it is not a major concern when you are only transferring 3.8 C, as was done in the miniature ET gun shots.

Figure 6 contains a photograph of one such modified switch mounted on a stand. It is only used in cases where overall circuit inductance is not a concern, typically at low current levels. Lower-inductance configurations are possible, however. ARL has successfully integrated a modified ST-300 switch with a 20-kV, 280-kJ bank in a relatively low-inductance configuration.

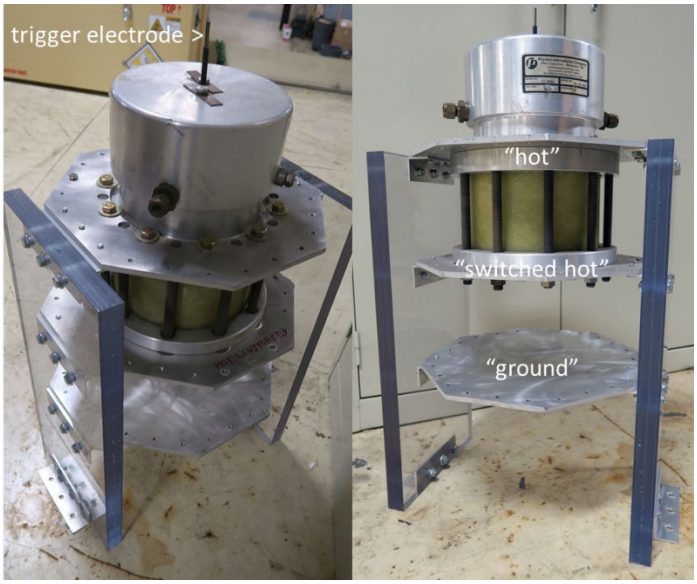


**Fig. 6 Modified L3 Communications Model ST300 spark gap switch**

One issue with the modified ST-300 switches is that they can no longer be pressurized, so the switch can no longer be optimized for different operating voltages. The general rule of thumb is that the operating voltage should be 2/3 to 3/4 of the breakdown voltage of the gap between electrodes. In the ST-300 the gap is 0.25 inches (6.3 mm) and has a breakdown voltage of approximately 22 kV at ambient pressure, so the preferred operating range is 15 to 16.5 kV at ambient pressure. In that range the switch delay time will be a small fraction of a microsecond, and the jitter (i.e., the random variation in the switch delay time) will be a small fraction of the delay time.

As the operating voltage drops below this preferred range, the delay time and the jitter increase in a highly nonlinear, power-law fashion, resulting in multi-microsecond delays at the lowest end of the operating range. That said, there are many applications where switch delay is of no concern, and we have operated these switches at voltages as low as 2 kV.

At ARL, the Trigatron versions of the ST-300 switch are operated in the "mode A" configuration, which is to say that the trigger pulse has a positive polarity and the trigger electrode is inserted in the positive electrode.[8] This mode purportedly yields the best delay times and the widest operating range. An ARL-designed isolation transformer, pictured in Fig. 7, is used to isolate the 4-kV trigger unit from the 20-kV bank. One advantage of the use of a transformer is the ability to change the polarity of the trigger pulse merely by flipping the polarity of the output connections (as seen on the right in Fig. 7) if the 4-kV trigger unit has an inappropriate polarity.

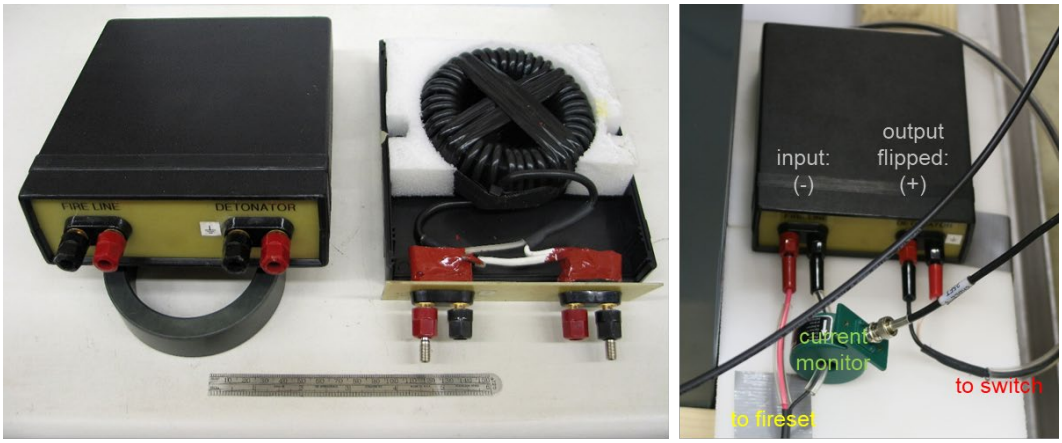


**Fig. 7 ARL-designed trigger pulse isolation transformer**

The transformer consists of a length of RG-58 coaxial cable wound around a ferrite ring with a 3.75-inch (95.2-mm) outer diameter. The core of the cable forms the primary, and the braid of the cable forms the secondary. For safety purposes all

such transformers are regularly tested to 30 kV. These transformers are often used near experiments involving explosives, and none have failed to date. This design was shown to exhibit good transfer efficiency when 4-kV EBW trigger pulses were used. Air core transformers were found to be less effective.

## 3.2 Spark Gap Electrode Design

While the graphite electrode design used in the ST-300 switch was likely to be much larger than what was required to survive the pulses used in the ET gun work, it was decided to use electrodes of that width so as to not constrain the width of the arc (and thus its inductance and resistance) and to allow for some off-center arc migration if the J × B forces on the arc were not perfectly balanced. Figure 8 contains a photograph of two of the graphite electrodes used. Like the ST-300 electrodes, they are 2.75 inches (70 mm) in diameter. Unlike the ST-300 electrodes, which are press-fit, ARL's electrodes are designed to be bolted to a flat plate by way of a pair of 3/8-16 threaded holes.


**Fig. 8 Graphite electrodes used in the ARL spark gap switch (scale in millimeters)**

## 3.3 Spark Gap Electrode Testing

A test article was built so that the electrodes could be mounted in a simple, unrefined spark gap switch configuration for testing purposes. The test article was then used to connect the second-generation capacitor bank to various dummy loads. Figure 9 contains a drawing of the test article, which consists primarily of two square aluminum plates separated by insulating spacers. This test article allowed for initial testing of the electrodes and gave the ability to measure the breakdown voltages of various gap sizes (which is not feasible when a switch is attached to a capacitor bank). Connections were made via threaded holes on the edges of the plates. The main flaw in this switch is the inherently asymmetric current feed

design. The plates were made 12 inches (305 mm) wide so that current spreading would alleviate that issue somewhat.

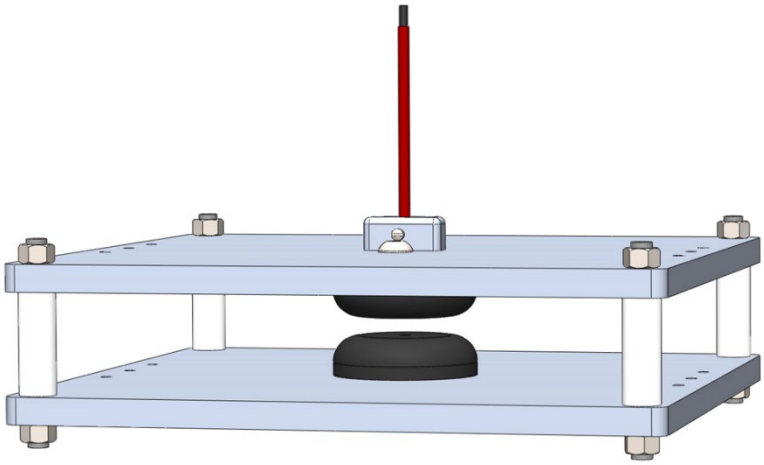

**Fig. 9 Graphite electrode test fixture**

Four loads were used in this initial testing: 1) nominally 130-mΩ resistive, 2) nominally 38-mΩ resistive, 3) simple exploding wire (EW), and 4) the switch by itself, acting as a short. All connections were made with lengths of 101-mm-wide × 0.5-mm-thick insulated copper strips. Table 1 lists the charge voltage used ($V_0$) and the peak currents achieved ($I_{max}$) in each experiment. A nominally 0.375-inch (9.5-mm) gap was used in all of these experiments. The breakdown voltage of the gap was 28 kV, so the switch was nominally optimized for operating voltages in the 19- to 21-kV range.

**Table 1 Results of electrode test fixture experiments**

| Load | $V_0$ (kV) | $I_{max}$ (kA) | $L_{tot}$ (nH) |
|---|---|---|---|
| 130 mΩ | 10 | 55 | 520 |
| | 15 | 87 | 520 |
| | 17 | 99 | 520 |
| | 20 | 118 | 530 |
| 39 mΩ | 20 | 218 | 540 |
| | 20 | 210 | 610 |
| EW | 20 | 339 | 530 |
| Switch only | 10 | 297 | 180 |
| | 13 | 358 | 200 |
| | 13 | 342 | 230 |
| | 14 | 357 | 245 |
| | 15 | 369 | 264 |
| | 16 | 369 | 300 |

The total inductance ($L_{tot}$) seen in each experiment, as determined by a fit to an inductance-resistance-capacitance (*LRC*) circuit model, is also listed in Table 1. This is included to give an indication of how well the positive and negative current feeds were kept taped or clamped together from one experiment to the next. The repulsive magnetic forces between the leads varies as the current squared, so for peak currents above 200 kA it became difficult to keep them from separating. After each experiment it became increasingly hard to reform the feeds into their original shape due to work hardening of the copper.

The switch delays measured should not be considered intrinsic, as no attempt was made to set the trigger unit to exactly 4 kV each time. That said, switch delays at 20 kV varied from 0.15 to 0.18 μs. The 15-kV shots had delays of 1.12 and 1.32 μs.

In the case where the switch itself was the load, no attempt was made to reclamp the copper strip conductors between experiments, so the total circuit inductance increased significantly from shot to shot. Figure 10 includes before and after pictures from that test series. The copper leads were nearly ripped off by the last shot despite being clamped in the middle and taped elsewhere. The last two shots achieved nearly 370 kA despite the ever-increasing inductance.

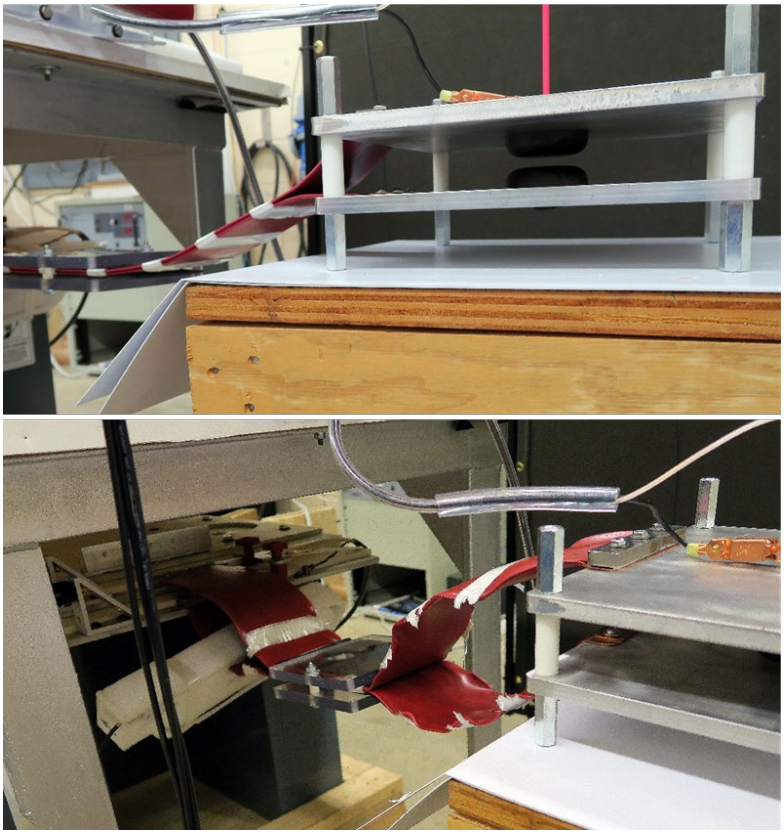

**Fig. 10 Photographs taken before (top) and after six experiments in which the switch itself was the load**

Figure 11 contains a current-versus-+time plot for the 15-kV switch-only shot alongside the results of an *LRC* circuit simulation meant to fit the data. The fitted total resistance of 3 mΩ is typical of all the shots in the switch-only test series.

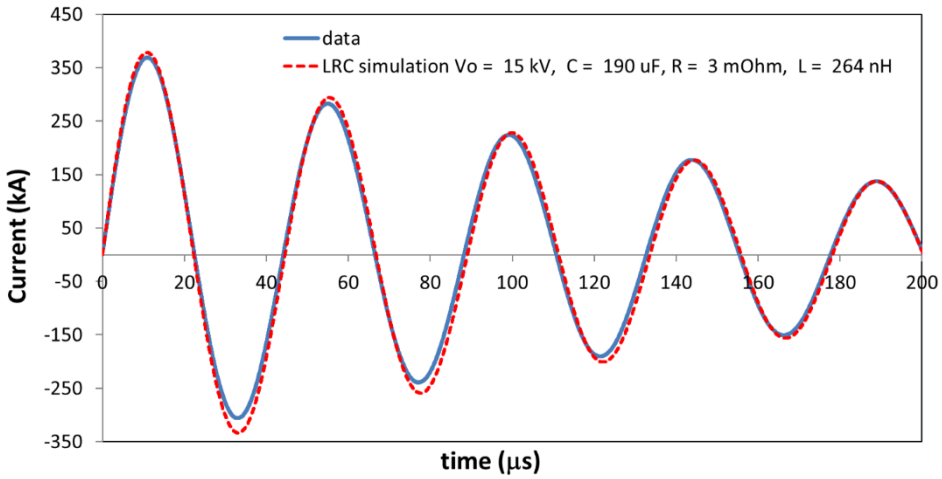


**Fig. 11 Current data from the 15-kV switch-only experiment compared with the results of an *LRC* circuit simulation**

Figure 12 contains a photograph of the negative electrode used in the test fixture after initial electrode testing was complete. While there was virtually no damage to the graphite electrode, the pattern of discoloration on the graphite indicates that most of the arcs formed off-center. Light arc damage is also visible on the aluminum mounting plate to the right of the graphite electrode. This is a consequence of the asymmetric current feeds. While the shifting of an arc from graphite to aluminum does not affect the operation of the switch significantly, it is still a maintenance issue, as the sprays of molten aluminum may end up compromising the insulating spacers. That said, it is not difficult to replace the insulating spacers.

**Fig. 12 Negative graphite electrode after initial testing**

While it was never intended to be a general-purpose spark gap switch (due to the issues associated with the asymmetrical current feeds), the electrode test fixture was successfully used in outdoor experiments involving single-barrel ET launchers. That particular arrangement achieved 410-kA peak current, the highest current ever achieved in any miniature ET gun experiment at ARL.

## 3.4 Capacitor Bank Header Design

The plan was to develop a triplate header configuration that included a spark gap switch, conformed to ARL Weapons and Materials Research Directorate's traditional header design rules, and met all of the novel requirements that this particular situation called for.

There were a number of design goals that had to be met. The two goals that drove the desire to incorporate the switch into the bank itself were the need to keep parasitic inductance below a certain level and the need to tightly control the geometry of the current feeds into and out of the switch so that there would be no net J × B force acting on the arc. The first requirement called for short connection structures, and the second complicated those connection structures by requiring a degree of symmetry. It was decided that the two requirements could best be met by making the connecting structures part of the capacitor bank header itself.

Having to balance the currents out of each of the three capacitors complicated the interconnection scheme further. That specification requires that the inductance of the current paths between each HV stud and the switch be the same or at least close. Unfortunately, the inductance of arbitrarily shaped structures is not easy to calculate, especially if they are confined between two ground planes. We resorted to a low-order approximation here.

It was decided to include a further goal: minimize the volume of the capacitor bank as much as possible. This was an outgrowth of the unfortunate size of the ICAR capacitors (large capacitor banks tend to be inconvenient). To meet this goal it was arbitrarily decided to aim for a header design that was no wider than a single capacitor.

The length of the header was determined by other considerations, in particular the requirement that the horizontal component of the "creepage" between all HV structures and all ground structures be a minimum of 2 inches (50.8 mm). Creepage is the technical term for the path length an arc must take to get from a point at high potential to one at low potential if it hugs the surface of the intervening insulator. While an air gap slightly larger than 6 mm will hold off 20 kV, arcs form much

more readily along surfaces, so larger separations are called for when insulating surfaces lie between high and low potential points.

This means that the hot plate must have 2 inches of clearance around all 12 of the aluminum bushings that connect the top ground plate to the bottom ground plate (one for each of the mounting bolts) as well as 2 inches of clearance to the outer edges of the header. This limits the space available for HV interconnections considerably. Note that 2 inches of horizontal creepage is far from conservative; it assumes that the insulating layers are kept clean and dry at all times.

The hot-plate design that was settled on is pictured in Fig. 13. This design maintains a symmetrical capacitor layout with the capacitors just far enough apart to allow the HV interconnections to fit within the 2-inch horizontal creepage requirement. Current is carried into the switch from two sides via 2-inch-wide conductors, which lead to the two side capacitors. Current is carried straight out of the switch to the output connection point by a relatively wide "switched-hot" plate. Hence, there should be little or no net J × B force on the arc coming from any of those connections.

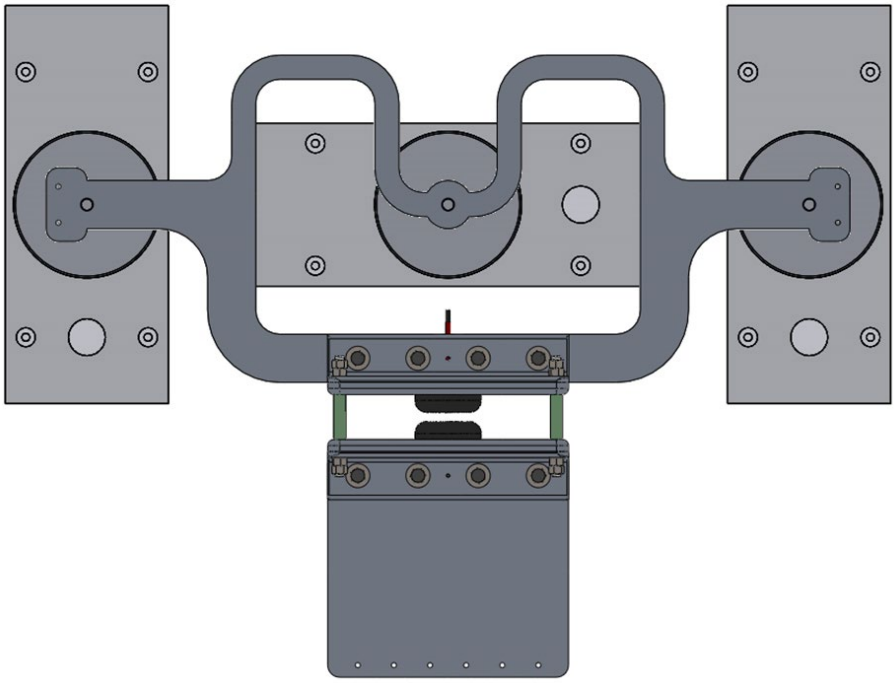

**Fig. 13 Hot plate and spark gap switch configuration (top view)**

The most complicated HV connection is the one to the central capacitor. To maintain symmetry, current must flow out of it in both the left and right directions. The two paths to the switch must be identical and the total inductance of the two

paths (essentially two identical inductors in parallel) must at least roughly equal the inductance of the path from one side capacitor to the switch.

As a first attempt it was decided to make the two outputs off the center capacitor 1 inch (25.4 mm) wide in keeping with the use of 2-inch-wide output connections on the side capacitors (ending with a net 4 inches at the switch). At that point it was just a matter of getting the path lengths right while filleting every corner appropriately.

Rounding the corners of conductive paths in high-current, HV systems is standard practice. Inside corners are rounded because, in a pulsed system, current tends to hug inside corners and that leads to localized heating if the inside corners are sharp. Outside corners are rounded because sharp outer corners concentrate the local electric field, inviting breakdown at those locations.

In the drawing depicted in Fig. 13, the convoluted connections to the middle capacitor are as long as the creepage requirement, header width requirement, and corner filleting choices will allow.

The shape of the path the current must follow in traveling from one of the side capacitors to the switch is indicated by the line labeled “path S” in Fig. 14. The shape of one of the two paths from the center capacitor to the switch is approximated by the combination of the lines labeled “path C1” and “path C2”. The estimated inductances of the associated conductor segments are referred to as $L_S$, $L_{C1}$, and $L_{C2}$, respectively. The total inductance between the center capacitor and the switch is referred to as $L_C$, defined by $L_C = ½(L_{C1} + L_{C2})$.

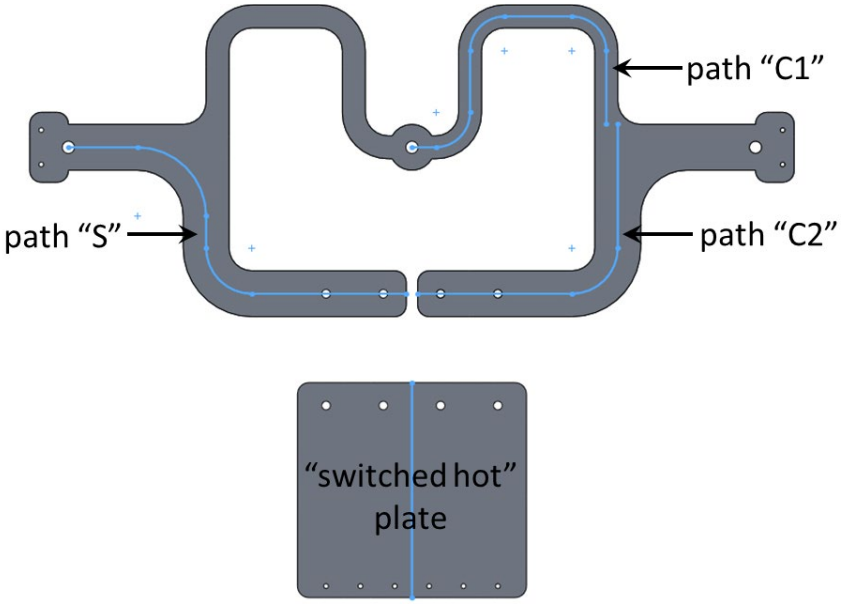


**Fig. 14 Centerlines used to approximate the lengths of specific current paths**

An approximation was used to estimate the relative magnitudes of the inductances of these paths, which is all that is needed to balance the individual currents. The approximation does not accurately represent the absolute magnitudes of the inductances; it only attempts to accurately recreate their ratios.

As a simplifying assumption, the presence of the ground planes above and below the conductors is ignored. The various bends in the conductors are also ignored. It is assumed that neither of those factors will affect the *relative* magnitudes of the inductances significantly. Thus, the problem devolves to calculating the inductances of straight bars with rectangular cross sections.

There are many equations used to estimate the inductance of a straight bar of rectangular cross section.[9] Each is generally accurate over a specific range of length/width ratios[9] (all tend to be accurate at high length/width ratios). Here we make use of one of the simplest equations[9,10]:

$$L = \frac{\mu_0 l}{2\pi}\left[\ln\left(\frac{2l}{a+b}\right) + \frac{1}{2}\right] \quad (1)$$

where $L$ is the inductance of the bar, $\mu_0$ is the permeability of free space, $l$ is the length of the bar, $a$ is the width, and $b$ is its thickness. In the situation depicted in Fig. 14, the thickness $b$ of each path is 3/8 inch (9.5 mm) and the width $a$ of each path is either 2 inches (50.8 mm) or 1 inch (25.4 mm). The lengths of each path, as derived from the original CAD drawing, are S = 482.3 mm, C1 = 431.0 mm, and C2 = 387.7 mm.

Applying Eq. 1, the individual inductance estimates work out to be $L_S$ = 315.7 nH, $L_{C1}$ = 319.5 nH, and $L_{C2}$ = 236.8 nH. One side of the center capacitor connection then has an estimated inductance of $L_{C1} + L_{C2}$ = 556.3 nH, and both sides in parallel have half that: $L_C$ = 278.1 nH. While this is not exactly equal to $L_S$ = 315.7 nH as was desired, it was deemed close enough (partly due to a lack of faith in the accuracy of the approximation). As the resistances of these paths are negligible, the current drawn from each capacitor will be inversely proportional to the inductance between it and the switch. Hence, the center capacitor will be the one to take a slightly higher burden if the approximation is correct. The expected fraction of current coming from the each capacitor is

$$center\ capacitor\ fraction = \frac{1/278.1}{2/315.7 + 1/278.1} = 0.36 \quad (2)$$

and

$$side\ capacitor\ fraction = \frac{1/315.7}{2/315.7 + 1/278.1} = 0.32 \quad (3)$$

The capacitor bank header was designed so that individual Rogowski coils could be embedded in the insulation surrounding the HV studs of the side capacitors so as to measure the current coming out of each of the side capacitors. The data from those, along with data from the Rogowski coil surrounding the load feed, allowed for a measurement of the true fraction of current supplied from each capacitor. As luck would have it, the fractions turned out to be 36%, 32%, and 32%, exactly as estimated.

Future versions of this bank could have a better current balance if desired. The most effective way of improving the balance would be to lengthen the 1-inch-wide conductor sections, as narrowing them is a less effective way of increasing their inductance. If the approximation is to be believed, path C1 would have to grow from 431 to 510 mm long. This would result in a header about 40 mm wider than the current header design if the length of the header was kept constant.

Figure 15 depicts the overall configuration of the capacitor bank. Figure 16 shows the capacitor bank in the laboratory. In the photograph on the left in Fig. 16, the Rogowski coil that measures the current from the foremost capacitor is clearly visible. The foam structure enclosing the load (an insulated loop of copper strip) contains a similar Rogowski coil. In the photograph on the right, the fiberglass tubes that space the two electrode mounting plates apart are covered by disposable sections of plastic sheet to protect the spacers from arc products. These plastic sheets incur very little damage in a single shot and will likely last many shots. Since the switched-hot output plate floats mechanically in its insulating sheathe, the gap size can be adjusted by varying the length of the fiberglass spacers. Alligator clips seen on the right in the photograph in Fig. 16 connect to the trigger pulse isolation transformer.

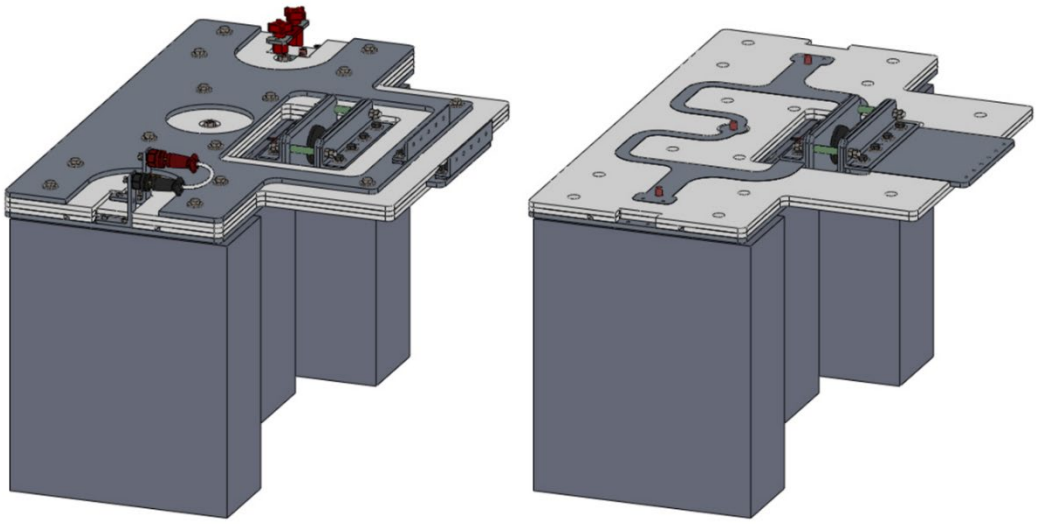

**Fig. 15 Final capacitor bank with spark gap switch design**

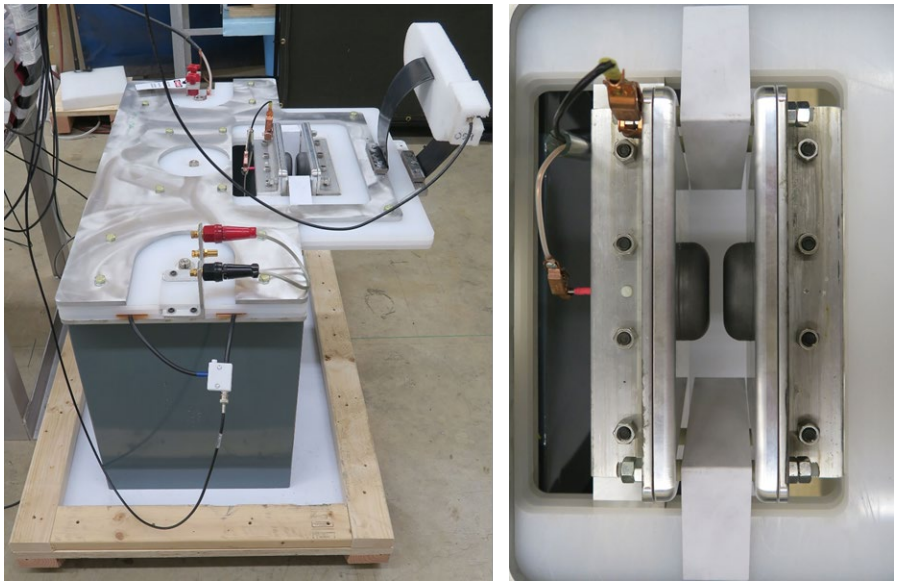

**Fig. 16 Final design**

Unlike the first- and second-generation banks' "stair-stepped" output sections, this bank's two ground outputs are parallel to one another (i.e., the lower one is a mirror image the upper one) because all current feeds must have a symmetry that balances the J × B forces on the arc.

As a circuit element, ARL's miniature ET gun resembles a two-electrode spark gap switch[1–3] in that it forms an open circuit until it is overvolted. It has been found that the switched-hot output plate on this bank floats up to a high voltage prior to firing, due to leakage currents, until the ET gun gap discharges the tiny amount of charge that has accumulated on the switched-hot plate (i.e., the static electricity it has acquired). Then the switched-hot plate floats up again and further discharges occur. As these tiny discharges contain very little energy, no harm is done; however, in some situations it may be wise to connect the switched-hot plate to ground via a high-value HV resistor to bleed off the static charge that develops and maintain the switched-hot plate at a low potential.

## 3.5 Capacitor Bank Testing

As the end goal of this effort was to prove that the switch could deliver peak currents on the order of 400 kA, the bank was tested with low-resistance inductive loads consisting of single loops of copper strip like the one seen in Fig. 16. Loops of two different sizes were used. The first consisted of a 4-inch-wide, 0.020-inch-thick annealed copper sheet 33.5 inches long from connection point to connection point (i.e., 101 mm wide, 0.5 mm thick, and 851 mm long). Two experiments were

performed with this load. The initial charge in the first experiment was 10 kV, which resulted in a peak current of 175 kA. Current data from that experiment are plotted in Fig. 17 along with the results of a fit to an *LRC* circuit model. The second experiment used an initial voltage of 20 kV, which resulted in a peak current of 354 kA. Current data from that experiment are plotted in Fig. 18.

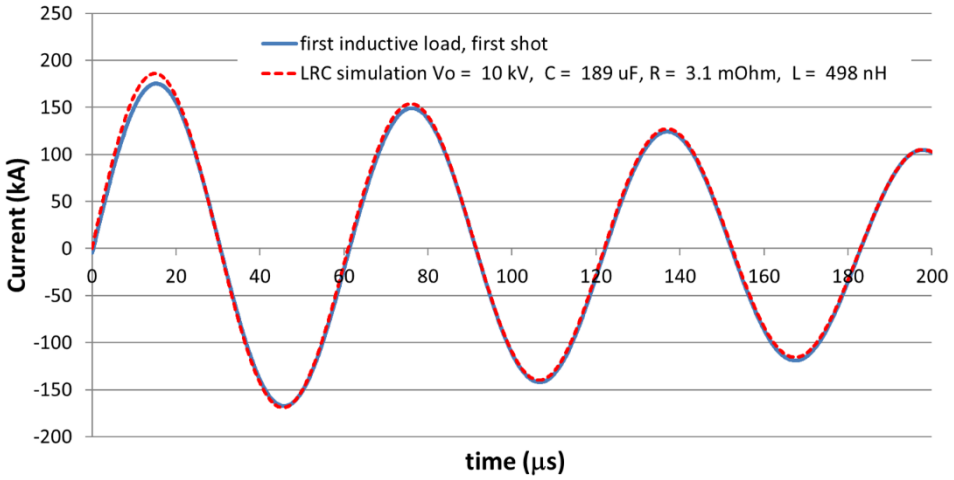


**Fig. 17 Results of the first inductive load experiment**

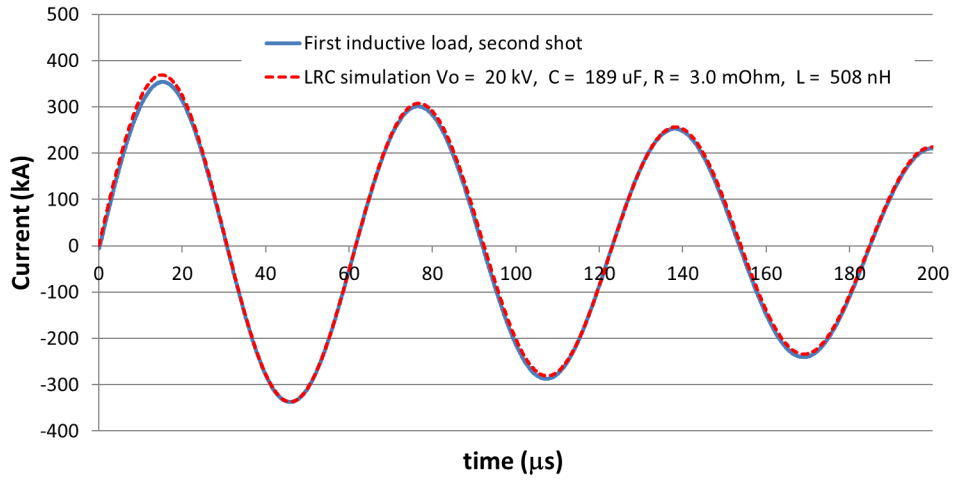


**Fig. 18 Results of the second inductive load experiment**

As the goal was to meet or exceed 400-kA peak current, a second, lower-inductance load was then constructed. It consisted of a 5-inch-wide, 0.020-inch-thick annealed copper strip 28.5 inches long from connection point to connection point (i.e., 127 mm wide, 0.5 mm thick, and 724 mm long). This experiment used an initial voltage of 20 kV, and resulted in a peak current of 411 kA. Current data from this experiment are plotted in Fig. 19 alongside a fit to an *LRC* circuit model.

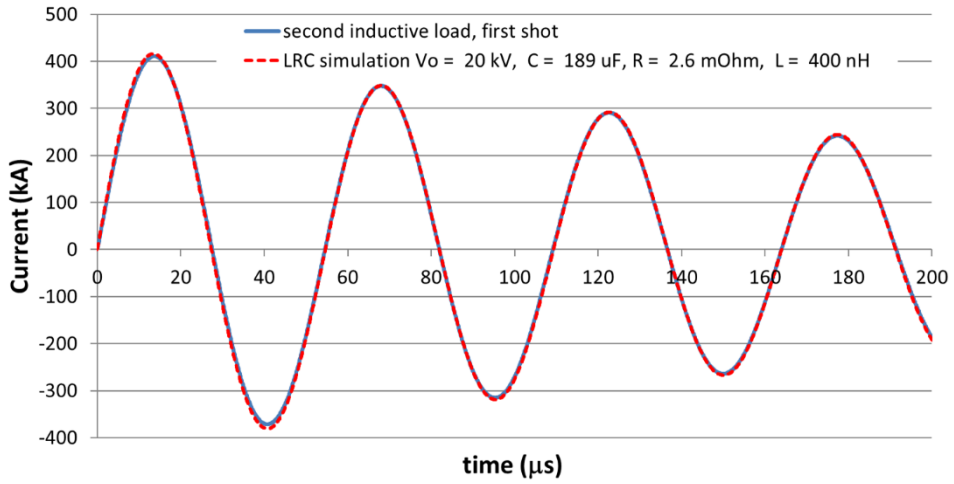


**Fig. 19 Results of the third inductive load experiment**

The reason that more experiments were not performed using these loads is made evident by the posttest photographs seen in Fig. 20. The left photograph shows the first inductive load after its 20-kV shot, and the right photograph shows the second inductive load after its 20-kV shot. The first load is cupped along its length and ripped at the clamp edges. The second load is ripped at the score lines in the copper that were made when the heat-shrink covering was trimmed with a utility knife. Neither load would have survived one more shot.

**Fig. 20 First inductive load (left) and the second inductive load (right) after testing**

In theory, if one knows the inductance of both of these loads, one can extract the parasitic inductance of the bank and switch combination based on the lumped inductance derived from the *LRC* fits, and if these were perfectly circular coils, it would be a simple matter. The inductance of a circular strip of rectangular cross section is given by Eq. 4[11]:

$$L = 0.002\pi^2 \left(\frac{2a}{b}\right) aK \quad (4)$$

where $L$ is the inductance of the loop in microhenries, $a$ is the mean radius of the loop in centimeters, $b$ is the width of the strip in centimeters, and $K$ is a function of the ratio $(2a/b)$. Values of this function can be found tabulated in Grover.[11] The difficulty here is that the strips seen in Fig. 20 do not form perfect circles due to the way they are mounted and the way the ground and HV connections are offset. The overall loops are best described as teardrop-shaped.

As there is no simple formula for the inductance of a teardrop-shaped loop, we resorted to an approximation: we assumed that the teardrop-shaped loop has the same inductance as a circular loop of the same cross-sectional area. Using a CAD drawing of the loops to determine their areas, we estimated that the first inductive load has an inductance of roughly 380 nH and the second inductive load has an inductance of roughly 250 nH. This turns out to be equivalent to assuming that the loops are circular and have a circumference that is the length of exposed portion of copper strip plus approximately 4.5 inches (114 mm), which is in keeping with the header and end connections' geometries.

Subtracting the estimated loop inductances from the lumped inductance values listed in Figs. 17–19 yields three estimates of the parasitic inductance of the capacitor bank and switch: 118, 128, and 150 nH, respectively. The average of the three estimates is 132 nH. This would appear to be sufficiently low to meet the requirement that the overall circuit inductance in single-barrel ET gun experiments be kept between 270 and 350 nH.[1,2]

While the inductive load experiments successfully demonstrated that the power supply had a sufficiently low inductance and could deliver peak currents in excess of 400 kA, this type of load proved to be problematic in that the magnetic fields generated by the loads were large enough to drag the arc off of the graphite electrodes. Evidence of this can be seen in the postshot photograph of one of the electrodes in Fig. 21, where clear arc damage can be seen on the bottom of the aluminum backing plate.

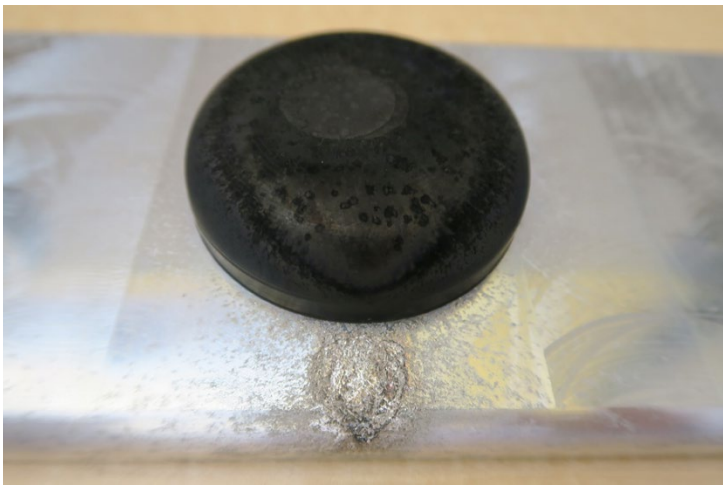

**Fig. 21 Evidence of J × B forces acting on the arc in the spark gap switch**

Another downside to low-resistance inductive loads is that they allow for large current reversals. This is yet another source of damage to the metallization in the capacitor and thus it should be avoided whenever possible.

It was then apparent that for general testing purposes it would be convenient to have a dedicated, noninductive dummy load that only drew modest currents and thus would not cause significant damage to the copper leads, spark gap switch, or capacitors. Such a load would allow for testing switch-delay times and operating ranges when different spark gap widths were set without causing damage to the system or the load.

The result is pictured in Fig. 22. It consists of four HVR APC Model W1528C0R1K silicon-carbide washer resistors (HVR Advanced Power Components, Inc, Cheektowaga, New York) in a series-parallel configuration. Each washer resistor is 152 mm in diameter, 25.4 mm thick, and is rated for up to 110 kJ of energy absorption in a single pulse. Each has a nominal resistance of 0.1 Ω, which is also the nominal resistance of the load itself. The actual resistance of the load was determined to be 0.107 Ω, measured with a DC milliohmmeter.

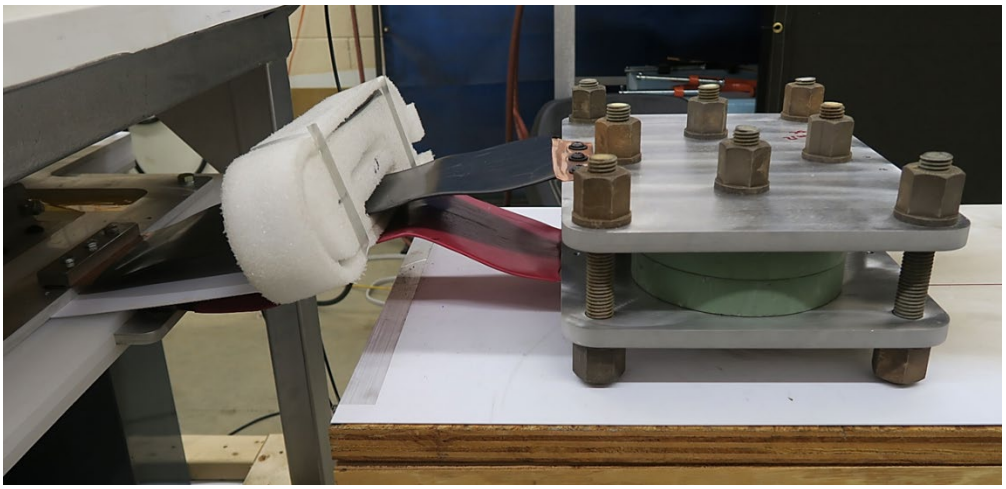

**Fig. 22 Dedicated resistive dummy load for power supply testing**

At 20 kV the load draws a peak current of 141.5 kA, as illustrated in Fig. 23. The switch-delay time in that experiment was 170 ns.

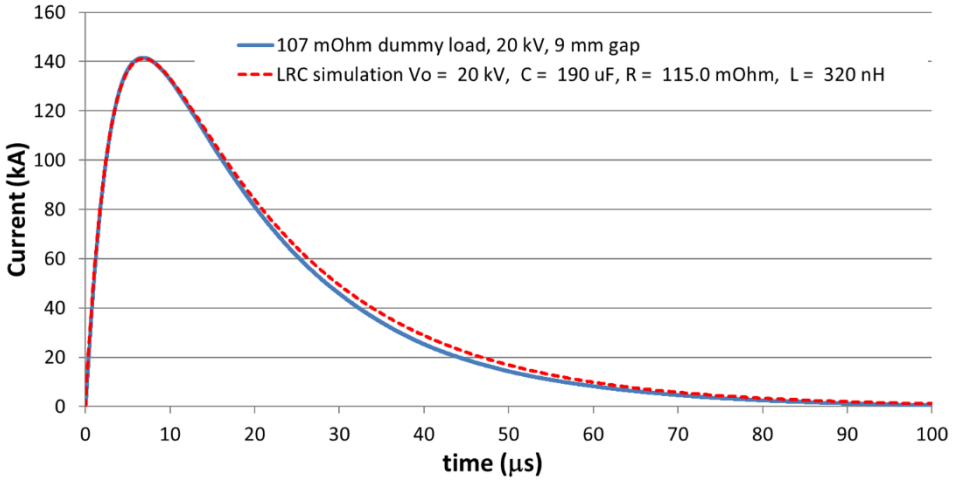


**Fig. 23 Current pulse derived using the dedicated dummy load**

Ultimately, this capacitor bank and switch arrangement proved its worth in an experiment where it powered a six-barrel ET gun design (Fig. 24). It achieved a peak current only slightly lower than a previous six-barrel experiment using the second-generation power supply and the mechanical switch. Projectile velocities measured in the two experiments were virtually equivalent.[3]

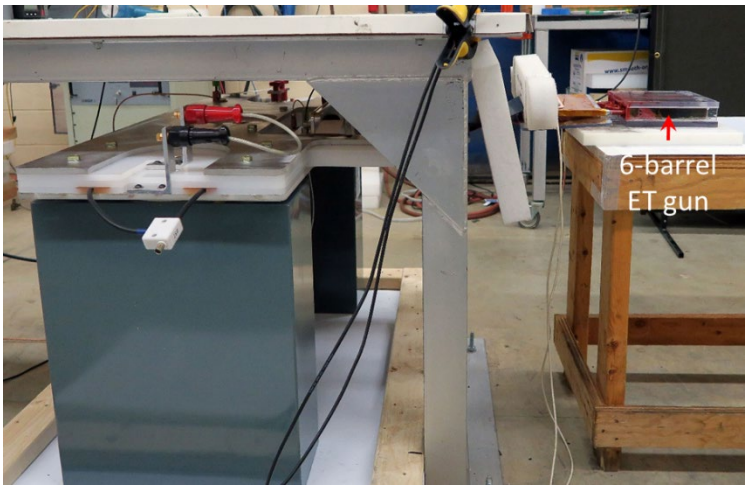


**Fig. 24 Capacitor bank attached to a miniature six-barrel electrothermal launcher**

## 4. Conclusion

We successfully designed, built, and demonstrated a capacitor bank design with an integrated spark gap switch that is suitable for supplying the high-current, short-period pulses that ARL's miniature ET guns and ET gun arrays require. A method was presented to design the conductor inductances to balance the flow of current from each capacitor. We demonstrated that the parasitic inductance of the design is within the desired range and that the spark gap switch can survive multiple pulses in the 350- to 400-KA range. While the current balance between the three capacitors in the capacitor bank is adequate for this application, we have identified a means of improving that balance in a future design.

## 5. References


1. Bartkowski P, Berning P, Uhlig WC, Coppinger MJ. Electrical arc-driven hypersonic projectiles. Aberdeen Proving Ground (MD): CCDC Army Research Laboratory (US); 2019 Apr. Report No.: ARL-TR-8683.

2. Uhlig WC, Bartkowski P, Berning P, Coppinger MJ. Controlling chamber expansion in miniature electrothermal guns for increased velocity and efficiency. Aberdeen Proving Ground (MD): CCDC Army Research Laboratory (US); 2019 June. Report No.: ARL-TR-8722.

3. Uhlig WC, Berning PR, Coppinger MJ, Bartkowski PT, Halsey ST. Small arrays of electrothermal launchers for hypervelocity millimeter-sized particles. Aberdeen Proving Ground (MD): CCDC Army Research Laboratory (US); 2020 July. Report No.: ARL-TR-8996.

4. Ennis JB, MacDougal FW, Yang XH, Cooper RA, Seal K, Naruo C, Spinks B, Kroessler P, Bates J. Recent advances in high voltage energy capacitor technology. Proceedings of the 16th IEEE International Pulsed Power Conference; 2007. p. 282–285.

5. Rabuffi M, Picci G. Status quo and future prospects for metallized polypropylene energy storage capacitors. IEEE T Plasma Sci. 2002;30(5):1939–1942.

6. Li L, Longjun X, Yunlong L, Xibo F, Chaobin B, Liu Y, Fuchan L. Development of a long-lifetime spark gap switch and its trigger generator for 2.0-MJ capacitive pulsed power supply module. IEEE T Plasma Sci. 2013;41(5)1260–1266.

7. Zeng H, Lin F, Cai L, Li L, Zhou Z, Qi X. Study of the erosion mechanism of graphite electrode in two-electrode spark gap switch. Rev Sci Instrum. 2012;83:013504.

8. Lehr J, Ron P. Foundations of pulsed power technology. Hoboken (NJ): John Wiley and Sons; 2017.

9. Piatek Z, Baron B, Szczegielniak T, Kusiak D, Pasierbek A. Self inductance of long conductor of rectangular cross section. Przegląd Elektrotechniczny (Electrical Review). R 88 NR 8/2012. p. 323–326. ISSN 0033-2097.

10. Kalantarov PL, Tseitlin LA. Inductance calculations (in Russian). Saint Petersburg (Russia): Energiya; 1970.

11. Grover FW. Inductance calculations. Mineola (NY): Dover Publications; 2004.

## Appendix. ICAR Bioenergy Model D 65-B 62.5-2000 Capacitor Specifications

ICAR S.p.A. – Via Isonzo 10 - 20900 Monza (MB) – ITALY

# *BIOENERGY D-65B 62.5-2000*

## *ENERGY STORAGE / DISCHARGE CAPACITOR*

## Self-healing metallized dielectric, impregnated with vegetable oil, NON-PCB dielectric fluid

### GENERAL CHARACTERISTICS

| | | |
|---|---|---|
| Rated Capacitance | µF | 62.5 |
| Capacitance Tolerance | % | ± 5 |
| Rated Voltage | kVdc | 20 |
| Test Voltage | kV | 22 |
| Rated Energy at rated voltage | kJ | 12.5 |
| Nominal Discharge Current | kApeak | 130 |
| Fault Discharge Current (max 3 times in the life) | kApeak | 200 |
| Nominal Voltage Reversal | % | ≤ 20 |
| Fault Voltage reversal (max 3 times in the life) | % | ≤ 70 |
| Maximum Integral Action ($\int i^2dt$) | MJ/ohm | 0.2 |
| Fault Integral Action | MJ/ohm | 0.8 |
| Maximum RMS Current | Arms | 50 |
| Maximum discharge repetition rate | | 1 discharge / 2 min |
| Tangent of the loss angle (tan δ) @ 100V - 50Hz by Schering bridge | | $\leq 1 \cdot 10^{-3}$ |
| Equivalent series resistance (ESR) | mΩ | ≤ 2.5 |
| Equivalent series inductance (ESL) | nH | ≤ 60 |
| Dielectric | | Self-healing metallized polypropylene |
| Dielectric Fluid | | vegetable oil |

**Life Expectancy with the a/m duty cycle and 95 % reliability**

| | | |
|---|---|---|
| shot life | shots N. | ≥ 1000 |
| dc life | hours | ≥ 300 |
| end of life | | Internal failure or Capacitance < 95 % of the initial value |

### ENVIROMENTAL and OPERATING CHARACTERISTICS

| | | |
|---|---|---|
| Climatic category : | | |
| Lowest operating temperature | °C | -10 |
| Maximum operating temperature | °C | +40 |
| Lowest storage temperature | °C | -25 |
| Maximum storage temperature | °C | +65 |
| Humidity | % | ≤ 95 |
| Cooling | | NATURAL |
| Operating position | | Upright or Horizontal |

**MECHANICAL CHARACTERISTICS**

| | | |
|---|---|---|
| Dimensions | | SEE DRAWING 4K12468 Rev.A |
| Case material | | STAINLESS STEEL |
| Case colour | | GREY RAL 7031 |
| Bushings number | | 1 |
| style | | Low profile |
| Terminals | | Metric M12 x 38 mm stud |
| Maximum tightening torque | N·m | 25 |
| Clamping nuts | | 4 x Metric M10 x 15 mm deep |
| Weight | kg | about 54 |

**ROUTINE TEST (100% of the units)**

Visual and Dimensional Control

Voltage Test between terminals at 22 kVdc for 10s, at room temperature

Capacitance and Tangent of Loss Angle Measurement by Schering Bridge at 1000 V, at room temperature

N.3 Discharge in short circuit with 20 kV Charge Voltage, at room temperature

Sealing Test at 65°C for 20 hours

**DRAWING**

4K12468 Rev.A : BIOENEREGY D-65B 62.5-2000 - Outline Dimensions

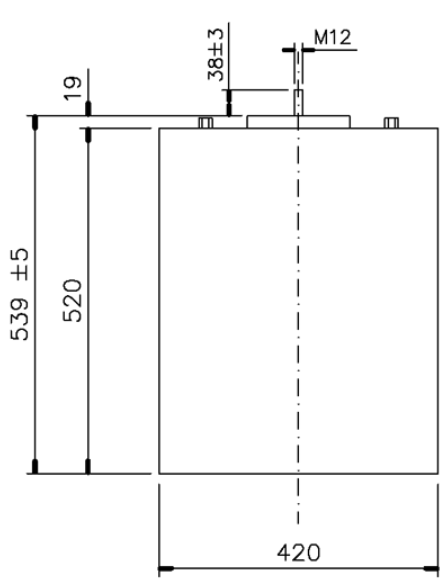


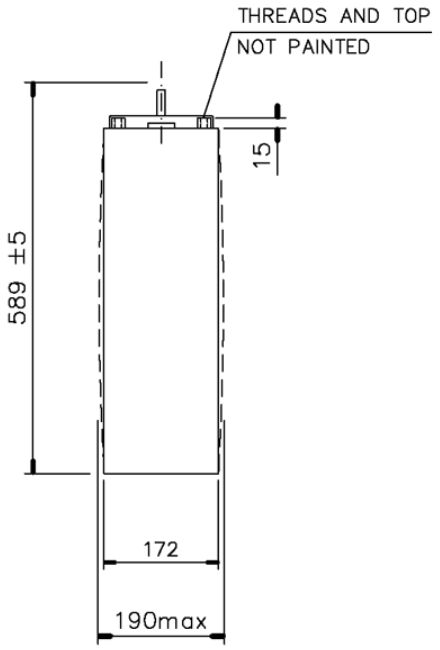


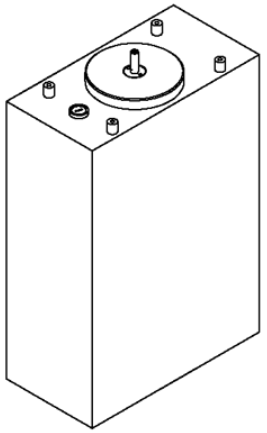

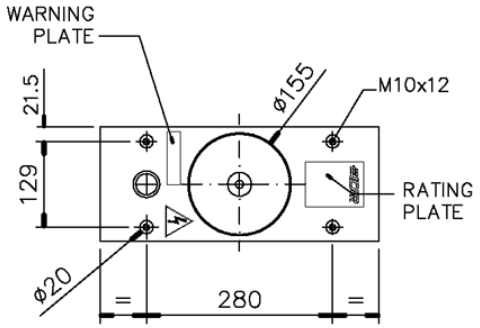


Dimensions in mm
Threads metric
Case material Stainless Steel
Weight approx 54 kg
Contain approx 16 $dm^3$ of vegetable oil

| Rev. | Descrizione Revisioni / Revision Description | Data/Date | Firma/Sign. | Approv. |
|---|---|---|---|---|
| A | PRIMA EMISSIONE | 28/6/16 | F.G. | |

ICAR INDUSTRIA CONDENSATORI APPLICAZIONI ELETTROELETTRONICHE

Disegno/Drawing: 4K12468– Rev. A

Titolo / Title: ENERGY STORAGE / DISCHARGE CAPACITOR
BIOENERGY D–65B 62,5–2000
62,5 µF ±5% – 20 kV – 125 kJ

Foglio/Sheet | Segue/Follow | Centro di Costo: 1 2 3 / 4 5 6 / 7 8 9

Scala/Scale: 1.5



Sostituito dal N. / Replaced by N.
Sostituisce il N. / Replaces N.

Per quote senza indicazione di tolleranza vedasi norme UNI ISO 2768 classe di tolleranza c / For dimensions without tolerance indication refer to UNI ISO 2768 class of tolerance c

## List of Symbols, Abbreviations, and Acronyms

| | |
|---|---|
| AC | alternating current |
| ARL | Army Research Laboratory |
| B | magnetic flux density |
| CAD | computer-aided design |
| CCDC | US Army Combat Capabilities Development Command |
| DC | direct current |
| EBW | exploding bridge wire |
| ET | electrothermal |
| EW | exploding wire |
| GA | General Atomics |
| HV | high voltage |
| $I_{max}$ | peak currents achieved |
| J | surface current density |
| $L_{tot}$ | total inductance |
| *LRC* | inductance-resistance-capacitance |
| nH | nanohenry |
| PP | polypropylene |
| RFQ | request for quote |
| UV | ultraviolet |
| $V_0$ | charge voltage used |

1 (PDF) DEFENSE TECHNICAL INFORMATION CTR DTIC OCA

1 (PDF) CCDC ARL FCDD RLD CL TECH LIB

2 (PDF) LANL L NEUKIRCH J BRADLEY

24 (PDF) CCDC ARL FCDD RLW P R FRANCART D LYON P BARTKOWSKI FCDD RLW PA S BILYK J FLENIKEN T KOTTKE M MCNEIR C WOLFE P BERNING M COPPINGER W UHLIG L VANDERHOEF A VALENZUELA B WILMER J NESTA D MALONE M GREENFIELD FCDD RLW PD B KRZEWINSKI A BARD R DONEY G VUNNI M ZELLNER FCDD RLW PE P SWOBODA D SCHALL